Pore nucleation in mechanically stretched bilayer membranes

Zun-Jing Wang[a] and Daan Frenkel
Fundamenteel Onderzoek der Materie (FOM), Institute for Atomic and Molecular Physics, Kruislaan 407, 1098 SJ Amsterdam, The Netherlands

(Received 24 June 2005; accepted 16 August 2005; published online 14 October 2005)

We report a computer-simulation study of the free-energy barrier for the nucleation of pores in the bilayer membrane under constant stretching lateral pressure. We find that incipient pores are hydrophobic but as the lateral size of the pore nucleus becomes comparable with the molecular length, the pore becomes hydrophilic. In agreement with previous investigations, we find that the dynamical process of growth and closure of hydrophilic pores is controlled by the competition between the surface tension of the membrane and the line tension associated with the rim of the pore. We estimate the line tension of a hydrophilic pore from the shape of the computed free-energy barriers. The line tension thus computed is in a good agreement with available experimental data. We also estimate the line tension of hydrophobic pores at both macroscopic and microscopic levels. The comparison of line tensions at these two different levels indicates that the "microscopic" line tension should be carefully distinguished from the "macroscopic" effiective line tension used in the theoretical analysis of pore nucleation. The overall shape of the free-energy barrier for pore nucleation shows no indication for the existence of a metastable intermediate during pore nucleation. © *2005 American Institute of Physics*. [DOI: 10.1063/1.2060666]

The formation of pores in bilayer membranes plays a role in many biological and biomimetic systems.[1–3] The simplest model for pore formation in membranes is based on classical nucleation theory (CNT).[4] In this picture, the formation of pores in membranes is an activated process that is controlled by the competition between the surface tension of the membrane and the line tension associated with the rim of the pore. Based on this model, several theoretical investigations have been carried out to analyze the structural and dynamical properties of pores in membranes.[5–10] In order to observe pore formation in realistic models for phospholipid bilayers[11] on the time scale of a simulation (nanoseconds), very large stresses (or very large electric fields) are required. Coarse-grained simulations offer the possibility to perform a systematic study of the size and shape distribution of pores that appear spontaneously in a membrane at thermal equilibrium.[12] Using such studies, it is possible to estimate the line tension associated with the rim of the pore,[13] and the free-energy profile of pore formation in a membrane at constant surface area.[14] In parallel, there has been much progress in the development of experimental techniques to probe the dynamical features of pore formation in membranes.[15,16]

In spite of these efforts, our knowledge about the early stages of pore nucleation is still limited. Yet, experiments by Evans *et al.*[16] suggest that, precisely in this regime, something interesting happens. In Ref. 16, the rupture rate of spherical vesicles is probed as a function of the rate at which the tension is increased. These experiments suggest that pore nucleation is a two-stage process: presumably, in the early stages a molecular-size metastable defect forms that subsequently acts as the seed for the nucleation of a large pore. However, the experiments cannot provide direct information about the microscopic structure of this defect.

In the present study, we use Monte Carlo simulations to study the free-energy barrier for pore nucleation in stretched membranes. These simulations allow us to gain insight in the molecular arrangements in the membrane during the early stages of pore nucleation. All simulations were carried out at constant temperature and constant lateral tension. To limit the computational cost, we made use of a solvent-free coarse-grained membrane model that we had tested previously.[17] In the present study, we consider bilayer membranes consisting of 1152 lipid molecules.

As pore nucleation is an activated process, the spontaneous formation of pore nuclei in a moderately stretched membrane is infrequent. It can be invoked by a very high tension, but in this case, once a pore occurs, membrane rupture follows quickly.[11] As a consequence, "brute-force" simulations of pore nucleation will typically require unphysically large values of the membrane tension and, even then, very long simulation runs are often required.[11,13] To circumvent this problem, we use the umbrella sampling (see, e.g., Ref. 18) to compute the free-energy barrier for pore nucleation. The approach that we employed is similar to the one used in the numerical study of crystal nucleation.[19,20] The advantage of this Monte Carlo scheme is that it can be used to simulate pore nucleation under constant lateral stresses that are lower than those needed to observe membrane rupture in brute-force simulations. In fact, with the present approach we can, in principle, compute the pore-nucleation free-energy barriers at the relatively low tensions that are employed in experiments. Moreover, the present technique allows us to stabilize the pore nuclei of arbitrary size in order to analyze their structure.

[a]Electronic mail: wang@amolf.nl

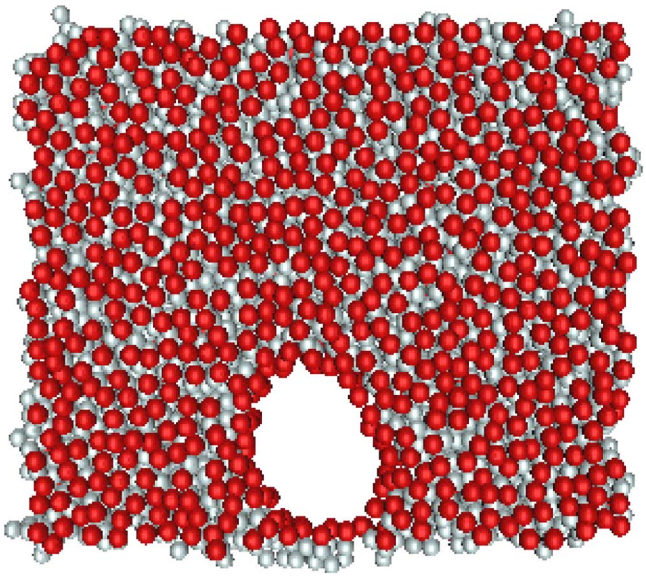

FIG. 1. Top view of a bilayer with a hydrophilic pore. The red spheres represent hydrophilic head groups and the gray spheres represent hydrophobic tail groups.

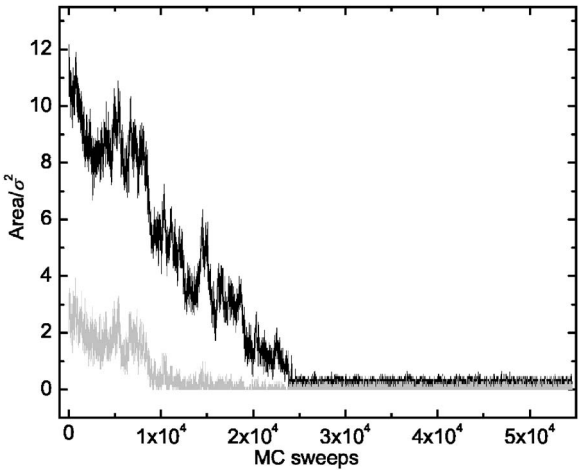

FIG. 2. Temporal evolution of the pore area during annealing of a preformed pore in a membrane under constant lateral stress ($\Sigma=4.0k_BT/\sigma^2$). The dark curve represents the area unoccupied by hydrophobic chains, and the light one indicates the area occupied by neither hydrophobic nor hydrophilic groups.

Free energies are only defined as a function of a variable that, depending on the context, is often referred to as a "reaction coordinate" or, as we will do in the remainder of this paper, an "order parameter." In our definition of the order parameter, we wish to make as few assumptions as possible about the structure of the incipient pore. In what follows, we use as order parameter the projected area of pores in the x-y plane (i.e., the plane of the bilayer membrane). To measure the pore area, we decorate the membrane with a square lattice with unit cells of $0.3\times0.3\sigma^2$, where σ is the hard-core diameter of hydrophobic tails of our model surfactants. A pore consists of a connected cluster of "empty" squares.

The advantage of this choice of order parameter is that it is insensitive to the precise shape of the pore. However, we still have to specify what we mean by empty squares. We have tested two different definitions: in one method, we designated a square as empty if it did not overlap with the (projected) excluded volume of any lipid. However, we found that with this definition, even with biased sampling, we were unable to make the pores grow. This suggests that this order parameter misses an essential aspect of the structure of incipient pores. In the second approach that we tried, a square was designated as empty if it did not overlap with the excluded volume of the hydrophobic part of any of the lipids. For a defect-free membrane, the two definitions are almost equivalent. However, the present definition allows for the formation of a defect where a pore opens in the hydrophobic part of the membrane, but not yet on the (hydrophilic) surface. With this definition of the order parameter, we were able to follow the progression from defect-free membrane to fully developed pore using our umbrella-sampling scheme.

In our simulations, we found both "hydrophobic" and "hydrophilic" pores. We refer to a pore as hydrophilic when its rim is covered with hydrophilic groups. In hydrophobic pores, the hydrophobic groups are exposed at the rim. Figure 1 shows a snapshot of a typical hydrophilic pore.

We used biased Monte Carlo simulations to generate pores of different sizes. In a number of cases, we performed unbiased simulations to study the time evolution of the pores thus generated. We verified that "precritical" pores (i.e., pores with a size less than the one corresponding to the maximum in the free-energy barrier) would spontaneously reseal and supercritical pores would spontaneously grow. Of course, pores with a free energy close to the maximum, could evolve in either direction. Figure 2 shows a typical example of the temporal evolutions of the pore area during an unbiased simulation at constant stress. The two curves correspond to the two definitions of the pore area. Interestingly, the figure shows that the hydrophilic part of the pore reseals well before the hydrophobic part. This figure illustrates why the definition of an order parameter that includes the hydrophilic part of the chains is not very useful; the hydrophobic defect anneals considerably later than the hole in the hydrophilic surfaces. During the time between $1\times10^4-2\times10^4$ Monte Carlo (MC) sweeps, the process involved in pore closure is still happening, but it is obviously not captured by taking the hydrophilic pore area as a reaction coordinate. Since in that region, the other reaction coordinate is still monotonously decreasing, we claim that the latter is a much better reaction coordinate.

All simulations (both with and without biased sampling) indicate that very small pore nuclei correspond to hydrophobic pores (see Fig. 3 left). When the size of the pore nucleus becomes comparable with the molecular length, the pore becomes hydrophilic, i.e., the rim of the pore becomes coated with hydrophilic head groups (see Fig. 3 right).

Figure 4 shows the measured free-energy landscapes relative to the pore-free state of the membrane. In this figure, R is a measure for the pore size. It is defined as $R\equiv\sqrt{A/\pi}$, where A is the area of the pore. We computed the free-energy landscape of pore nucleation for three different imposed stretching surface tensions: $\Sigma=4.0k_BT/\sigma^2$, $\Sigma=4.5k_BT/\sigma^2$, and $\Sigma=5.0k_BT/\sigma^2(k_BT=2.0\epsilon)$. In all cases, we verified that

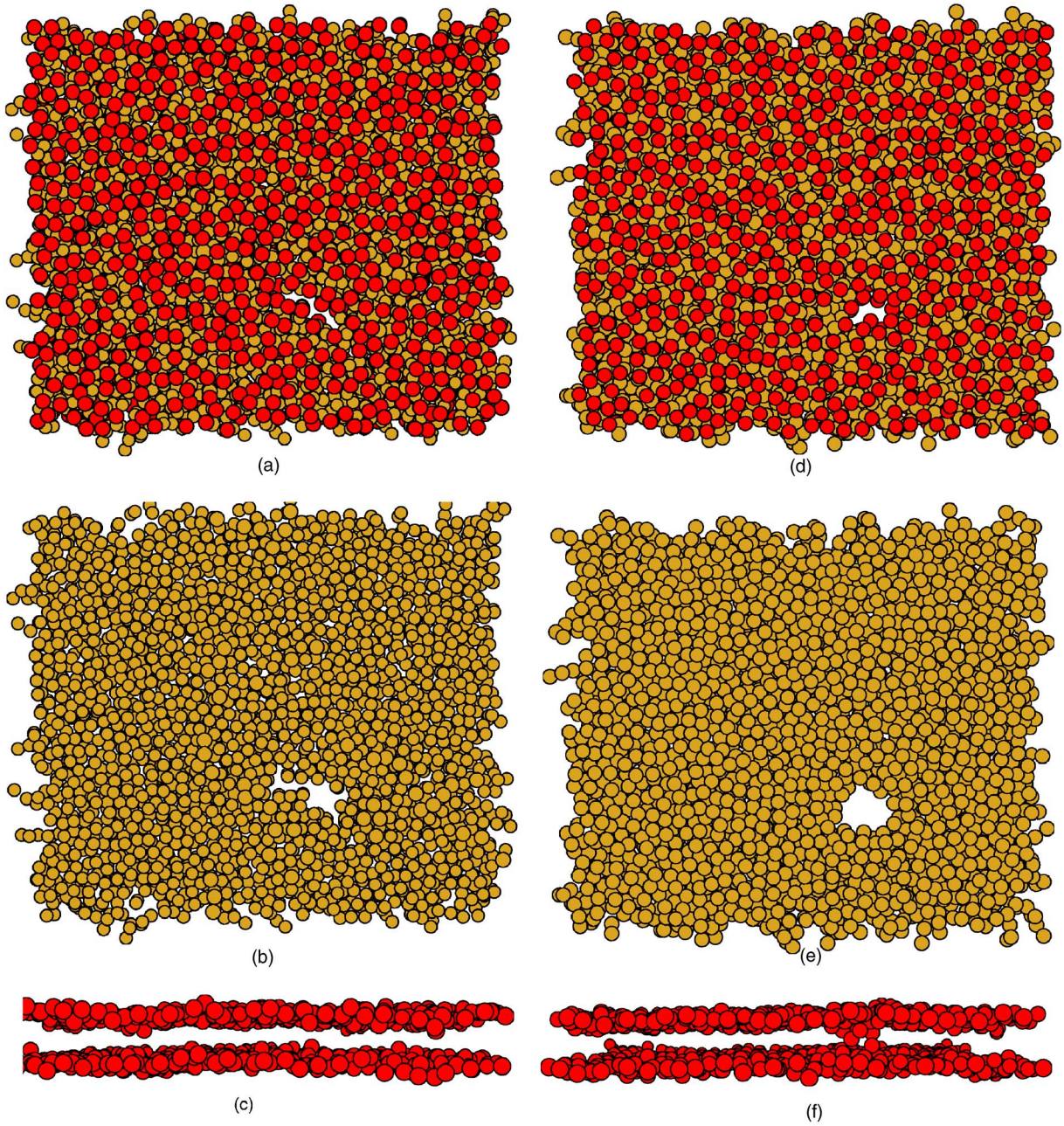

FIG. 3. Top and side views of bilayer membranes with a hydrophobic (left) and hydrophilic pore (right), respectively. In the figure, hydrophobic spheres are light (yellow) and hydrophilic spheres are dark (red). In the upper two top views [(a) and (d)], both hydrophobic and hydrophilic beads of amphiphiles are shown. In the middle two top views [(b) and (e)], only hydrophobic beads of amphiphiles are shown, where we can see that the hydrophobic pore (left) has a more rough shape than the hydrophilic pore (right). In the bottom two side views [(c) and (f)], only hydrophilic beads are shown. We can observe that for a membrane with a hydrophobic hole (c), the hydrophilic regions of the two monolayers are still isolated, while for a membrane with a hydrophilic hole (f), the hydrophilic beads of the amphiphiles in the rim of hole have moved into the hydrophobic region of the membrane and connected the hydrophilic parts of the two monolayers.

there was no hysteresis between pore opening and pore closing. The free energy for pore formation is obtained as follows: first we compute $n(R)$, the probability density to observe a pore with a radius between R and $R+\Delta R$, where $\Delta R=0.02\sigma$. This number was divided by N_L, the total number of lipids in the system. The free energy ΔG is then defined as $\Delta G \equiv -k_B T \ln(n(R)/N_L)$. In order to obtain the number of pores per unit membrane area, we should compute $\rho_L \exp(-\Delta G/k_B T)$, where ρ_L is the surface density of lipids.

Note that even for the largest tension shown in Fig. 4 [$\Sigma=5.0k_B T/\sigma^2$, which corresponds to $\mathcal{O}(20)$ mN in real units; see Ref. 17], the pore-nucleation barrier is at least $38k_B T$. Hence, the probability to observe the spontaneous formation of a "critical" pore in a system of 1152 lipids is extremely low [$\mathcal{O}(10^{-13})$]. Yet, this is the range of tensions where pore nucleation becomes observable in a macroscopic sample.

We can compare the computed nucleation barrier with the value predicted on the basis of classical nucleation theory (CNT):[4]

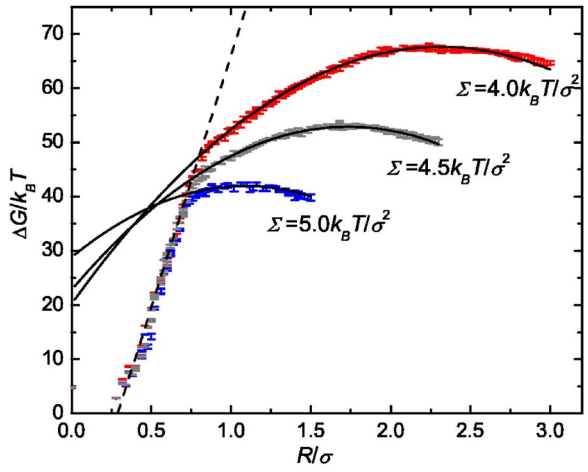

FIG. 4. Free-energy barriers for pore nucleation in model bilayer membranes. The three curves show the barriers for imposed surface tensions $\Sigma=4.0k_BT/\sigma^2$, $\Sigma=4.5k_BT/\sigma^2$, and $\Sigma=5.0k_BT/\sigma^2$. The free energy is measured in units of the thermal energy k_BT. The estimated error in the computed free energies is indicated by error bars. The dashed straight lines are fitted to the computed R dependence of the free energy of small hydrophobic pores. The solid curves represent fits of the computed free energy of large pores to the form predicted by CNT.[4]

$$G = G_0 + 2\pi R_c\Gamma - \pi R_c^2\Sigma, \tag{1}$$

where Γ is the line tension associated with the rim of the pore and Σ is the lateral tension of the membrane. R_c is the effective radius of a pore, defined as

$$R_c = \alpha R, \tag{2}$$

where α is a correction parameter for the radius of a pore, which is necessary since we have measured the area of pore A over discrete grids and have computed the radius as a function of A by assuming that the shape of a hydrophilic pore is a circle.

Independently fitting with Eq. (1) to the three free-energy landscapes of hydrophilic pores, we obtained the optimized parameters as shown in Table I. The line tensions at the applied surface tensions in this paper range between $4.6-7.8k_BT/\sigma$. By using the temperature and length scales defined before:[17] $\varepsilon/k_B \sim 150$ K and $\sigma \sim 5-8$ Å, the line tension of the simulated membranes is about 23–64 pN, which lies in the range of experimental data.[21–23]

Interestingly, when the pores are very small ($R<0.7\sigma$), the free energy is nearly a linear function of R. This indicates that the free energy of hydrophobic pores is dominated by the line free energy of the rim of the pore. In fact, the general shape of Fig. 4 is quite similar to the one deduced from the experiments of Ref. 21. The only conspicuous difference is that, in our simulations, we find no evidence for the existence of a metastable defect state at the end of the linear part of the free-energy barrier. Nevertheless, the qualitative agreement between experiment and simulation supports the notion that the early stage of pore nucleation involves the formation of a hydrophobic defect.

TABLE I. Parameters of the best CNT fits to the computed free-energy barriers for the nucleation of a hydrophilic pore in the membranes under constant lateral stretching pressures and room temperature ($k_BT=2.0\epsilon$).

$\Sigma/(k_BT/\sigma^2)$	G_0/k_BT	α	$\Gamma/(k_BT/\sigma)$
4.0	20.2	0.84	7.77
4.5	22.8	0.84	6.56
5.0	28.8	0.84	4.57

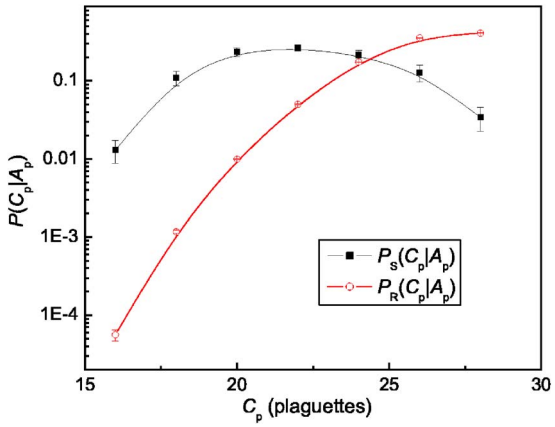

FIG. 5. Conditional distribution of the circumference of pores with a fixed pore area. The filled squares correspond to simulations of mechanically stretched membranes under conditions of constant surface tension $\Sigma/(k_BT/\sigma^2)=4.0$. The open circles are simulation results for the conditional circumference distribution of random pores with the same fixed pore area. In both cases, the area of pores A_p is fixed at $1.17\sigma^2$.

In our simulations, the height of the free-energy barrier for pore nucleation is of the order of $35-45k_BT$. This value is some two to three times larger than was estimated on the basis of the analysis on experimental data ($10-15k_BT$).[21] This discrepancy is not surprising in view of the special condition of the modeled membrane, even though this solvent-free model can reproduce elastic properties of biological membranes roughly within experimental range.[17] Suppose the theoretical analysis of experimental data is correct, there are still many factors which could lead to the quantitative difference of the free-energy barriers between simulations and experiments., e.g., the effect of impurities in experiments, the variations of solvent hydrophobicity and amphiphile molecular flexibility, the finite size of simulated membranes, etc.

Snapshots show that the shape of early hydrophobic defects is not circular but rough (see Fig. 3 left). This was also observed in the study of spontaneous pore formation in Ref. 12. To compute the free-energy cost associated with the rim of the pore, we study $P_S(C_p|A_p)$, the conditional distribution of pore circumferences C_p at fixed pore area A_p. We determine both the area and the circumference of a pore by "tiling" the pore with square plaquettes with an area of $0.3\times0.3\sigma^2$. The distribution of circumferences thus determined has both an energetic and an entropic contributions. We can estimate the entropic contribution by computing the circumference distribution of "random" pores with the same surface area A_p, $P_R(C_p|A_p)$. The computed conditional circumference distributions $P_S(C_p|A_p)$ and $P_R(C_p|A_p)$ for a fixed pore area A_p are shown in Fig. 5. The ratio between the two distributions is due to the line tension associated with the circumferences. Indeed, we find that $\ln[P_S(C_p|A_p)/P_R(C_p|A_p)]$ is a linear function of C_p (see Fig. 6). This suggests that, even for small, hydrophobic pores, it is meaningful to talk

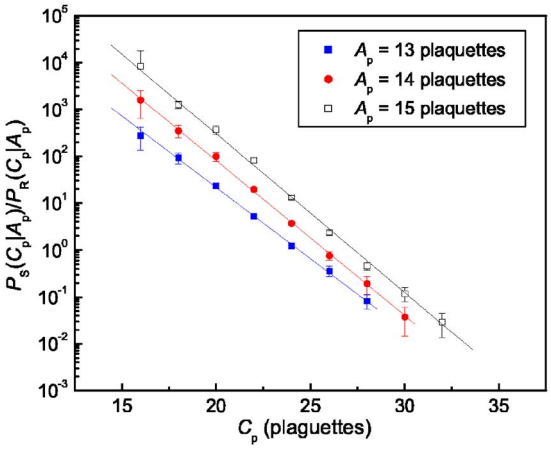

FIG. 6. Ratio of conditional distributions of the circumference of pores with a fixed pore area, $P_S(C_p|A_p)/P_R(C_p|A_p)$, for mechanically stretched membranes under conditions of constant surface tension $\Sigma/(k_BT/\sigma^2)=4.0$. The areas of pores are fixed at $1.17\sigma^2$, $1.26\sigma^2$, and $1.35\sigma^2$, respectively (pore size R as defined in Fig. 4, are separately 0.61σ, 0.63σ, and 0.66σ). From the slope of the semilog plot, we can estimate the "microscopic" line tension.

about a "line tension" of the pore. Moreover, the good quality of the linear fits in Fig. 6 implies that small pores are not intrinsically anisotropic: their deviation from a circular shape is exclusively due to thermal fluctuations. Fitting the data in Fig. 6 to $-k_BT\ln[P_S(C_p|A_p)/P_R(C_p|A_p)]=G_0+\Gamma_tC$, we obtain that the line tension of hydrophobic pores from thermal fluctuation is $\Gamma_t=0.70-0.78k_BT/l_p$, where l_p is the length per plaquette, i.e., $\Gamma_t=2.3-2.6k_BT/\sigma$. Interestingly, the above "microscopic" value of the line tension of a hydrophobic pore is very different from the value obtained by fitting the linear part in the free-energy curve of Fig. 4. The free energy of small pores can be written as $G=G_0+2\pi R\Gamma_e$, with $\Gamma_e=14.8k_BT/\sigma^2$. This effective line tension is a factor of six larger than the microscopic line tension Γ_t. This means that microscopic line tension can not be introduced into a "macroscopic" theory to estimate the free energy of pore nucleation.

In summary, we have computed the free-energy barriers of pore formation in bilayer membranes and compared them with the predictions of CNT. The simulations indicate that the pores are initially hydrophobic but, when they grow larger than the typical molecular scale, they become hydrophilic.

The free energy of hydrophilic pores is qualitatively described by classical nucleation theory. The line tensions extracted from the computed free-energy curves lie in the experimental range. Small pores are hydrophobic. They have irregular shapes, but are not intrinsically anisometric. The roughness of small pores is due to their small microscopic line tension. However, their effective line tension is quite large and completely dominates the free energy of incipient pores.

The work of the FOM Institute is part of the research program of the Stichting voor Fundamenteel Onderzoek der Materie (FOM), which is financially supported by the Nederlandse Organisatie voor Wetenschappelijk Onderzoek (NWO). One of the authors (Z.W.) thanks A. Cacciuto, C. Valeriani, and H. Tepper for helpful discussions. Computer time at the Dutch center for high-performance computing (SARA) is also gratefully acknowledged.

[1] B. Alberts, A. Johnson, J. Lewis, M. Raff, K. Roberts, and P. Walter, *Molecular Biology of the Cell*, 4th ed. (Garland Science, New York, 2002).
[2] R. Lipowsky and E. Sackmann, *Structure and Dynamics of Membranes from Cells to Vesicales* (Elsevier Science, Amsterdam, 1995).
[3] D. V. Zhelev and D. Needham, Biochim. Biophys. Acta **1147**, 89 (1993).
[4] J. D. Litster, Phys. Lett. **53A**, 193 (1975).
[5] D. Exerowa, D. Kashchiev, and D. Paltikanov, Adv. Colloid Interface Sci. **40**, 201 (1992).
[6] S. A. Freeman, M. A. Wang, and J. C. Weaver, Biophys. J. **67**, 42 (1994).
[7] J. C. Shillcock and U. Seifert, Biophys. J. **74**, 1754 (1998).
[8] M. Muller and M. Schick, J. Chem. Phys. **105**, 8282 (1996).
[9] P. R. Netz and M. Schick, Phys. Rev. E **53**, 3875 (1996).
[10] V. Talanquer and D. W. Oxtoby, J. Chem. Phys. **118**, 872 (2003).
[11] D. P. Tieleman, H. Leontiadou, A. E. Mark, and S.-J. Marrink, J. Am. Chem. Soc. **125**, 6382 (2003).
[12] C. Loison, M. Mareschal, and F. Schmid, J. Chem. Phys. **121**, 1890 (2004).
[13] T. V. Tolpekina, W. K. den Otter, and W. J. Briels, J. Chem. Phys. **121**, 8014 (2004).
[14] T. V. Tolpekina, W. K. den Otter, and W. J. Briels, J. Chem. Phys. **121**, 12060 (2004).
[15] O. Sandre, L. Moreaux, and F. Brochard-Wyart, Proc. Natl. Acad. Sci. U.S.A. **96**, 10591 (1999).
[16] E. Evans, V. Heinrich, F. Ludwig, and W. Rawicz, Biophys. J. **85**, 2342 (2003).
[17] Z. Wang and D. Frenkel, J. Chem. Phys. **22**, 234711 (2005).
[18] D. Frenkel and B. Smit, *Understanding Molecular Simulation: From Algorithms to Applications*, 2nd ed. (Academic, Boston, 2002).
[19] P. R. ten Wolde and D. Frenkel, Science **277**, 1975 (1997).
[20] S. Auer and D. Frenkel, Annu. Rev. Phys. Chem. **55**, 333 (2004).
[21] E. A. Evans and F. Ludwig, J. Phys.: Condens. Matter **12**, A315 (2000).
[22] S. Loi, G. Sun, W. Franz, and H.-J. Butt, Phys. Rev. E **66**, 31602 (2002).
[23] P.-H. Puech, N. Borghi, E. Karatekin, and F. Brochard-Wyart, Phys. Rev. Lett. **90**, 128304 (2003).